The King model for electrons in a finite-size ultracold plasma

2008 J. Phys. A: Math. Theor. 41 425501

(http://iopscience.iop.org/1751-8121/41/42/425501)

IOP PUBLISHING JOURNAL OF PHYSICS A: MATHEMATICAL AND THEORETICAL

J. Phys. A: Math. Theor. **41** (2008) 425501 (10pp) doi:10.1088/1751-8113/41/42/425501

The King model for electrons in a finite-size ultracold plasma

D Vrinceanu[1], **G S Balaraman**[2] **and L A Collins**[1]

[1] Theoretical Division, Los Alamos National Laboratory, Los Alamos, NM 87545, USA
[2] School of Physics, Georgia Institute of Technology, Atlanta, GA 30332, USA

Received 9 June 2008, in final form 27 August 2008
Published 29 September 2008
Online at stacks.iop.org/JPhysA/41/425501

Abstract
A self-consistent model for a finite-size non-neutral ultracold plasma is obtained by extending a conventional model of globular star clusters. This model describes the dynamics of electrons at quasi-equilibrium trapped within the potential created by a cloud of stationary ions. A random sample of electron positions and velocities can be generated with the statistical properties defined by this model.

PACS numbers: 36.10.−k, 32.80.Pj, 32.60+i

(Some figures in this article are in colour only in the electronic version)

1. Introduction

Ultracold plasmas (UCP) are obtained from a sample of atoms cooled by standard magneto-optical trap techniques and laser-excited just above the ionization threshold [1]. The excess energy, which can be varied from about 0.1 K to 100 K, is imparted to the free electrons which quickly leave the plasma. However, the trailing slow ions left behind create a net positive space charge that prevents further ejection of electrons. Therefore only a fraction of the electrons effectively leave the cloud; the value of this fraction depends on the number of atoms ionized. The remaining electrons reach a local quasi-equilibrium state within a short time, of the order of the electron plasma relaxation time, while the ions barely move, if at all, during this time. Since the most energetic electrons have already left the plasma, the remaining electrons cannot be described by a Maxwell–Boltzmann distribution, which includes electrons with arbitrarily large velocities. On a longer time scale, the cloud expands inducing an adiabatic cooling while the three-body recombination and de-excitation collisions tend to warm up the plasma.

Molecular dynamics (MD) simulations can accurately follow the dynamics of a UCP but only for a short time due to extreme computing requirements [2]. It is therefore important to start with a physically plausible configuration and to have the ability to scale the size of the system. Kuzmin and O'Neil [3] started their N-body simulation with a far-from-equilibrium distribution. A hybrid MD approach [1] uses the electronic quasi-equilibrium distribution as a

background for the ion motion at time steps greater than the electron relaxation time. Recent experiments [4] have measured the refilling rate of the Rydberg atom in a UCP at various times during its expansion as an indicator of the instantaneous electron temperature. At these times, a microwave flash re-ionizes the UCP, creating again the conditions for the electronic quasi-equilibrium.

The goal of this paper is to study the equilibrium distribution of electrons captured by a stationary ion cloud. A practical procedure for sampling the electron position and velocity random distribution is given, which consistently describes the system after the electron equilibration but before the start of expansion. Such distributions can be used as a starting point for MD simulations of initial expansion or refilling rates. Following suggestions from [5, 6], a productive analogy with the dynamics of globular star clusters can be employed to the benefit of UCP simulations. This field of astrophysics has a long history [7] and provides accurate models for the cluster dynamics, which is strikingly similar (evaporation, ejection, soft binaries, etc) to UCP dynamics. However, in contrast to the gravitational case, the attractive forces are counterbalanced by the repulsive forces between like particles, and the mass ratio for the particles in the system is very large. These two simple facts are the basis for important differences between the star clusters and UCP. Evidence that the electron distribution is different from a Maxwell–Boltzmann distribution was also discovered in [8].

The self-consistent distribution obtained by solving King's equation [9] was proved to provide a very accurate description for many globular clusters. Based on this success, a similar distribution was proposed in the seminal paper [10] to describe the electron distribution in UCP. The present paper further investigates this direction of research and explores the differences between King's equation and its solutions as applied in astrophysics and for UCP.

2. King electron distribution

We consider a spherically symmetric cloud of N_i heavy ions, clamped on their positions, with the Gaussian density,

$$\rho_i(\mathbf{r}) = \frac{N_i}{4\pi\sigma^3}\sqrt{\frac{2}{\pi}}\,\mathrm{e}^{-r^2/2\sigma^2},$$

where σ is the characteristic cloud size. The electric potential created by the ion cloud alone is the regular solution of the Poisson equation $\nabla^2\Phi_i = -\frac{e}{\epsilon_0}\rho_i$,

$$\Phi_i(\mathbf{r}) = N_i\frac{e}{4\pi\epsilon_0\sigma}\frac{\mathrm{erf}(r/\sqrt{2}\sigma)}{r/\sigma}.$$

A number $N_e \leqslant N_i$ of electrons move in the potential created by the ion cloud. Their stationary distribution cannot be Maxwell–Boltzmann (MB) since the potential Φ_i is finite as $r \to \infty$. The problem is that the electrons in the tail of the MB distribution, with large velocities, are able to escape the ionic trap. The King distribution was proposed [9] as a stationary solution for a self-gravitating globular cloud of stars. Electrons with a similar distribution have the phase-space density, as defined in [10, 11]:

$$f(\mathbf{r},\mathbf{v}) = \frac{\mathcal{N}}{(4\pi)^2 v_T^3\sigma^3}(\mathrm{e}^{-(E-E_0)/kT} - 1)\Theta[-e\Phi(0) \leqslant E \leqslant E_0], \tag{1}$$

where $\mathcal{N}$ is a normalization factor, $v_T = \sqrt{kT/m}$ is a characteristic velocity and k is the Boltzmann constant. Here T is a simple parameter, not the temperature, but related to the electron temperature in a way which will be revealed in section 5. The distribution depends on $\mathbf{r}$ and $\mathbf{v}$ coordinates only through the energy $E = mv^2/2 - e\Phi(r)$, which ensures that f is

a stationary solution of Liouville's equation. Note that here, $\Phi = \Phi_i + \Phi_e$ is the total electric potential, due to both the ions and electrons. In general, when $N_i > N_e$, the potential Φ is a positive, monotonically decreasing function of the radial coordinate r. The Θ function is 1 when its argument is true and 0 otherwise, and ensures that only electrons with energy less than the threshold energy $E_0 < 0$ are trapped. The negative threshold energy E_0 is related to the maximum spatial extension allowed for electron r_0, by $E_0 = -e\Phi(r_0)$. Similar to the globular cluster case, the spatial and energy truncation are necessary to describe systems which are not isolated, but in contact with weak external fields, such as the electric and magnetic fields used to collect charged particles. The limit of the King model for $r_0 \to \infty$, as discussed in the section 4, has an acceptable solution only for $N_e = N_i$. This means that an infinite size King model can only model a neutral plasma with the same number of electrons and ions. At a given radial position r, the escape velocity is defined as $v_e = \sqrt{2e(\Phi(r) - \Phi(r_0))/m}$.

In order to sample the distribution (1), we need to find first the potential Φ, and the relation between the size r_0, the threshold energy E_0, the normalization $\mathcal{N}$ and the number of electrons N_e. This goal is accomplished by solving the complete Poisson equation $\nabla^2\Phi = -\frac{e}{\epsilon_0}\rho_i + \frac{e}{\epsilon_0}\rho_e$, where the electron density is obtained by integrating the phase-space distribution over the velocity space

$$\rho_e(\mathbf{r}) = \frac{\mathcal{N}}{4\pi v_T^3\sigma^3}\int_0^{v_e} v^2\,\mathrm{d}v(\mathrm{e}^{-(E-E_0)/kT} - 1).$$

Changing the integration variable from v to x according to $v^2 = 2v_T^2[x + e(\Phi(r) - \Phi(r_0))/kT]$, we find

$$\rho_e(\mathbf{r}) = \frac{\mathcal{N}\sqrt{2}}{4\pi\sigma^3}\int_{-e(\Phi(r)-\Phi(r_0))/kT}^{0}\sqrt{x + e(\Phi(r) - \Phi(r_0))/kT}(\mathrm{e}^{-x} - 1)\,\mathrm{d}x,$$

which gives an implicit relation between ρ_e and Φ. By defining $W(r) = e(\Phi(r) - \Phi(r_0))/kT$, the electron density can be calculated by direct integration as

$$\rho_e(\mathbf{r}) = \frac{\mathcal{N}\sqrt{2}}{4\pi\sigma^3}\int_{-W}^{0}\sqrt{x + W}(\mathrm{e}^{-x} - 1)\,\mathrm{d}x = \frac{\mathcal{N}\sqrt{2}}{4\pi\sigma^3}\frac{2}{3}\left[\frac{3\sqrt{\pi}}{4}e^W\,\mathrm{erf}\sqrt{W} - (W + 3/2)\sqrt{W}\right] \tag{2}$$

This expression is valid only for $0 \leqslant r \leqslant r_0$, where $W \geqslant 0$, while outside this interval $\rho_e = 0$.

The function W is obtained as the solution of the complete Poisson equation when the electron density ρ_e is replaced by expression (2). As a result, the following nonlinear ODE has to be solved:

$$\frac{1}{R}\frac{\mathrm{d}^2}{\mathrm{d}R^2}RW(R) = -\frac{N_i}{N_0}\sqrt{\frac{2}{\pi}}\,\mathrm{e}^{-R^2/2} + \frac{\mathcal{N}}{N_0}\left[\sqrt{\frac{\pi}{2}}e^W\,\mathrm{erf}\sqrt{W} - \left(\frac{2}{3}W + 1\right)\sqrt{2W}\right], \tag{3}$$

where $R = r/\sigma$ is the normalized radial distance and $N_0 = 4\pi\epsilon_0 kT\sigma/\mathrm{e}^2$ is the characteristic particle number. The boundary conditions for this equation are: $W'(0) = 0$, $W(R_0) = 0$ and $W(R \to \infty) = -e\Phi(r_0)/kT$, where $R_0 = r_0/\sigma$.

Introducing the notation

$$\Sigma[W] = \begin{cases}\sqrt{\frac{\pi}{2}}\,\mathrm{e}^W\,\mathrm{erf}\sqrt{W} - \left(\frac{2}{3}W + 1\right)\sqrt{2W}, & W > 0\\ 0, & W \leqslant 0\end{cases}$$

the electron density is simply

$$\rho_e(r) = \frac{\mathcal{N}}{4\pi\sigma^3}\Sigma[W(r/\sigma)]$$

and the number of electrons is obtained by integrating (2) over the coordinate space

$$N_e = \mathcal{N} \int_0^{R_0} R^2 \Sigma[W]\, \mathrm{d}R.$$

Equation (3) is now written as

$$\frac{1}{R}\frac{\mathrm{d}^2}{\mathrm{d}R^2} R W(R) = -\frac{N_i}{N_0}\left(\sqrt{\frac{2}{\pi}}\, \mathrm{e}^{-R^2/2} - \alpha \Sigma[W]\right),$$

where the parameter α is introduced, such that $\mathcal{N} = \alpha N_i$.

This equation is very similar to the equation for the globular clusters, but there are important differences. The right-hand side in equation (3), unlike in the case of star clusters, is not always negative. The space scale in the plasmas is fixed by σ, whereas it is a model parameter for globular clusters. There is also no inhomogeneous term equivalent to the ionic contribution in plasmas, for the case of globular clusters.

3. Examples

In his seminal paper [9] King proposed to solve equation (3) by starting from the origin and integrating forward until $W = 0$. A class of models is therefore obtained for various values of the free parameter $W(0)$, the value of W at the origin.

As the right-hand side of equation (3) is always positive in the gravitational case, this procedure always yields a solution, and the cutoff radius R_0 for which $W(R_0) = 0$ increases with increasing $W(0)$. The plasma case is more complicated as the RHS of equation (3) can in principle be both positive and negative. The solution diverges if the RHS is positive, and hence not all values of $W(0)$ produce a meaningful model. Since the number of electrons N_e is related to distribution normalization, the number of electrons cannot be specified from the beginning, which is another serious drawback of this approach.

A better approach is to regard equation (3) as a boundary value problem, and to integrate it backward starting from R_0. This is facilitated by the observation that the solution to equation (3) is fully known outside the sphere of radius R_0, and has the expression

$$W_{\mathrm{out}}(R) = \frac{N_i}{N_0}\frac{\mathrm{erf}(R/\sqrt{2})}{R} - \frac{N_e}{N_0}\frac{1}{R} + \frac{E_0}{kT}, \qquad (R \geqslant R_0).$$

If N_i, N_e and E_0 are specified, then the cutoff radius R_0 is obtained as a solution of $W_{\mathrm{out}}(R) = 0$. Since the derivative of W is also known at R_0, then equation (3) can be integrated backward for various values of the normalization $\mathcal{N}$ (or α), with the goal of canceling the derivative at the origin: $W'(0) = 0$. This process is similar to the shooting method for solving boundary value problems.

Figure 1 illustrates three solutions obtained for a cloud of $N_i = 24\,000$ ions, of size $\sigma = 100\ \mu$m, and three different electron populations. The ion density falls down very fast (exponentially), while the electron density extends well outside the ion cloud, decreasing slowly to zero at R_0.

4. The case of no-space constraints

This section treats the case $R_0 \to \infty$. An integral equation is obtained from equation (3) by using Green's function for the Poisson equation and regarding the RHS as an inhomogenous term:

$$W(R) = \frac{N_i}{N_0}\frac{\mathrm{erf}(R/\sqrt{2})}{R} - \frac{\mathcal{N}}{N_0}\int_0^{\infty} \frac{x^2}{\max(x, R)}\Sigma[W]\, \mathrm{d}x, \qquad (4)$$

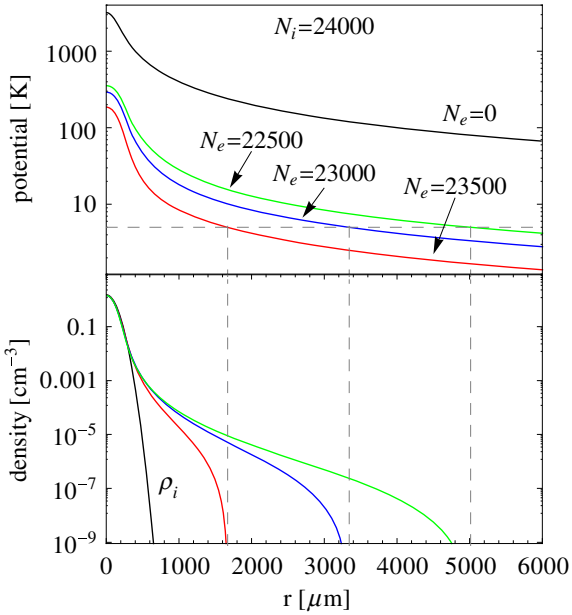

Figure 1. Three models with the same ion distribution with $N_i = 24\,000$ and $\sigma = 100$ μm, and different electron populations $N_e = 22\,500, 23\,000$ and $23\,500$. Parameters are $T = 50$ and $E_0 = -5$ K. Upper graph shows the electric potential along the radial direction. The lower graph shows the number density for electrons (color lines) and for the ions (black line). The potential created by the ions only is displayed in the upper graph (black line). The vertical dashed lines indicate the position of cutoff radius R_0 for each model, while the horizontal dashed line shows the threshold energy E_0.

where it is assumed that the integral makes sense, or in other words, $N_e = \mathcal{N}\int_0^\infty x^2\Sigma[W]\,\mathrm{d}x < \infty$.

The asymptotic behavior of the function Σ for small arguments is

$$\Sigma(x) = \frac{4\sqrt{2}}{15}x^{5/2} + \frac{8\sqrt{2}}{105}x^{7/2} + \mathcal{O}(x^{9/2}).$$

Therefore, a solution which decays only as $W \sim 1/R$, for $R \to \infty$, which would be obtained if the plasma were not neutral, is not acceptable because in that case Σ decreases as $\Sigma[W] \sim 1/R^{5/2}$, not fast enough to make the integral convergent.

If one assumes that $W(R) = A/R^\beta$, then the integral equation (4) for large R becomes

$$\frac{A}{R^\beta} = \frac{1}{R}\frac{N_i - \mathcal{N}\int_0^\infty x^2\Sigma[W]}{N_0} - \frac{\mathcal{N}}{N_0}\int_R^\infty x\left(1 - \frac{x}{R}\right)\Sigma[W]\,\mathrm{d}x.$$

For W to decay faster than $1/R$ it is required that $\beta > 1$ and that the coefficient in the $1/R$ term, proportional to total charge $N_i - N_e$, vanishes. On equating the LHS with the $1/R^{5/2\beta-2}$ from the second term on RHS, one gets $\beta = 4/3$, which is greater than unity as required.

If $N_e = N_i$, then one obtains the following constraint,

$$\frac{A}{R^{4/3}} = \frac{\mathcal{N}}{N_0}\frac{3\sqrt{2}}{5}\frac{A^{5/2}}{R^{4/3}},$$

which fixes the value of the normalization constant to

$$\frac{\mathcal{N}}{N_0} = \frac{5}{3\sqrt{2}A^{3/2}}.$$

Since the electron density is proportional to $\Sigma[W]$, and $W \sim 1/R^{4/3}$ at large R, then the electron density needs to decay as $\sim R^{-10/3}$. Such a model is obtained by starting at some value R_*, with the initial condition $W = A/{R_*}^{4/3}$ and integrating backward equation (3), toward the origin. The condition of regularity at the origin fixes the value of the only free parameter A.

5. Results

An ensemble of electrons with statistical properties in the (r, v) plane defined by equation (1) can be generated after obtaining the potential $\Phi(r)$ from the solution $W(R)$ of equation (3). Because the distribution is isotropic a full three-dimensional $(\mathbf{r}, \mathbf{v})$ population is obtained by attaching arbitrary directions to electron positions and velocities.

The King distribution in equation (1) is generated by first starting with an initial uniform distribution in the (r, v) plane and then performing Metropolis accept/reject steps until convergence. By denoting a point in the (r, v) plane by x, a proposed new point x' is obtained by sampling a random distribution which gives x' with probability $P_{x\to x'}$. A good choice for $P_{x\to x'}$ is, for example, a normal distribution centered at x and with the standard deviation a fraction of the (r, v) domain sampled. For this distribution $P_{x\to x'} = P_{x'\to x}$. The proposed $x \to x'$ step is accepted with the probability $\Omega_x(x') = \min(\rho(x')/\rho(x), 1)$, by generating a random number in the interval $[0, 1]$ and comparing it with the ratio $\rho(x')/\rho(x)$. The proposed step is accepted if the random number is less than $\Omega_x(x')$, or rejected otherwise. Here ρ is the desired distribution function given by equation (1). Therefore, the probability of moving point x to x' is $W_{x\to x'} = P_{x\to x'}\Omega_x(x')$. Since the detailed balance relation $\rho(x')W_{x'\to x} = \rho(x)W_{x\to x'}$ is satisfied, the initial distribution will converge to ρ after sufficient iterations.

The rest of this section will present a detailed analysis for a specific King model. This case has 25 600 ions and 25 088 electrons. The Gaussian ion distribution has standard deviation $\sigma = 120$ μm. The electron distribution has the parameter $T = 50$ K, threshold energy $E_0 = -5$ K and the cutoff radius $r_0 = 1711$ μm. The density in the center of the cloud for both electrons and ions is about 10^9 cm^{-3}. The electron distribution is obtained after 4000 Metropolis steps.

Figure 2 compares the radial distribution for electrons generated by the Metropolis random walk process with the prediction given by equation (2). The good agreement indicates convergence.

In figure 3, radial distribution of ions is compared with that of electrons. The electron distribution extends for larger distances and has lower densities at short distances.

The phase-space profile of the King distribution is shown in figure 4, where the contour lines indicate constant density. The left figure shows the sampled population while the figure on the right shows the predicted distribution of equation 1.

In figure 5, the velocity distribution for the sampled electrons can be seen to be in agreement with the theoretical prediction obtained by integrating distribution (1) over spatial coordinates

$$\rho(v) = \mathcal{N}\frac{v^2}{v_T^2}\left[\mathrm{e}^{-v^2/2kT}\int_0^{R^*(v)}\mathrm{e}^{W(R)}R^2\,\mathrm{d}R - \frac{R^*(v)^3}{3}\right],$$

where $R^*(v)$ is the radial position where $E = E_0$ for a given velocity. In contrast, the Maxwell–Boltzmann distribution, shown with the dashed line, extends for much larger velocities.

Although stationary, the King distribution is not characterized by a unique temperature. The symbol T in equation (1) is rather a parameter, and not the temperature. However, it is

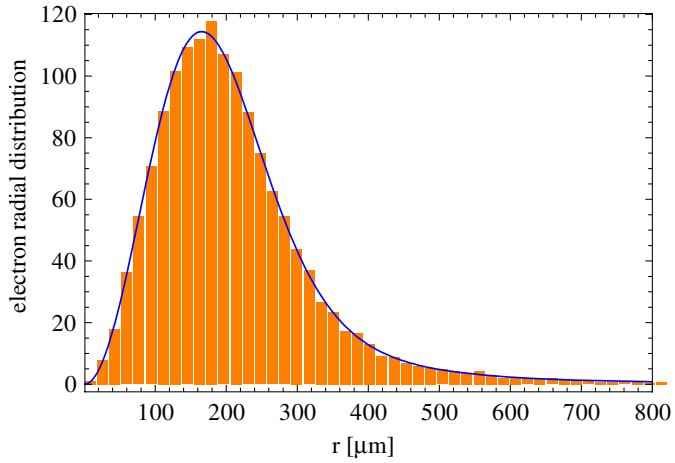

Figure 2. Electron radial distribution for the King distribution, from sampled population (histogram) and theoretical prediction (solid line).

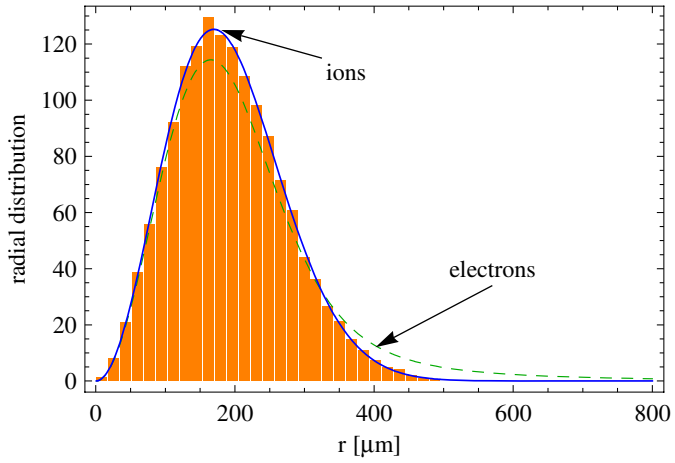

Figure 3. Ion radial distribution for the King distribution, from sampled population (histogram) and theoretical prediction (solid line), compared with electron radial distribution (dashed line).

possible to define a local temperature as a measure of the velocity dispersion: $T_{\rm local} = m\langle v^2\rangle/3$. This results in the following relation:

$$T_{\rm local}(R) = T\,\frac{\sqrt{\frac{\pi}{2}}\,{\rm e}^W\,{\rm erf}\sqrt{W} - \left(\frac{4}{15}W^2 + \frac{2}{3}W + 1\right)\sqrt{2W}}{\sqrt{\frac{\pi}{2}}\,{\rm e}^W\,{\rm erf}\sqrt{W} - \left(\frac{2}{3}W + 1\right)\sqrt{2W}},$$

where W is the solution of equation (3). Figure 6 compares the predicted position-dependent temperature with the temperatures sampled inside regions separated by a series of spherical shells.

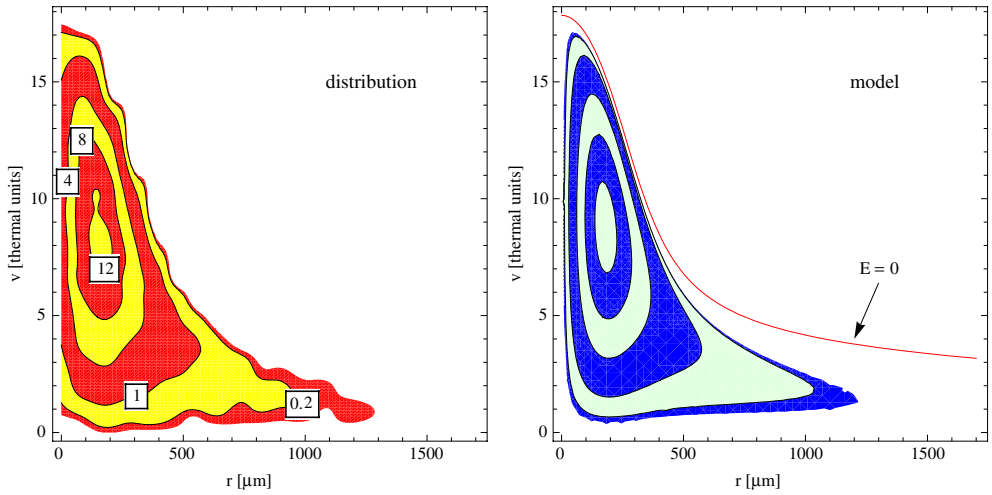

Figure 4. Phase-space distribution for the King electron distribution. The contour lines are lines of equal density. The run-away ($E = 0$) curve is shown in the right panel. The unit for velocity is $\sqrt{k_B K/m}$, where k_B is the Boltzmann constant and m is the electron mass.

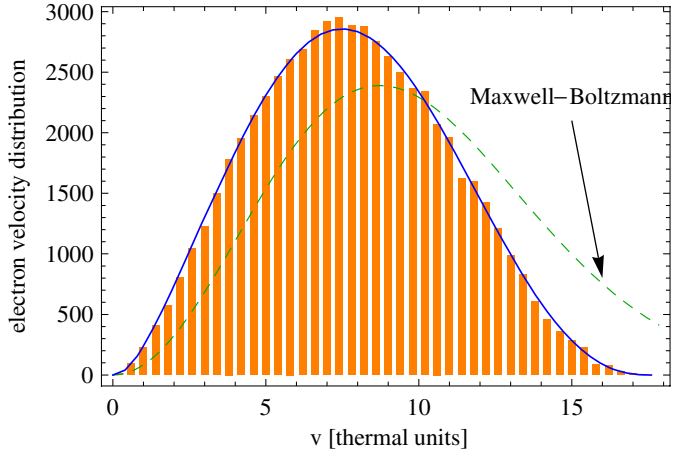

Figure 5. The electron velocity for the King distribution from the sample (histogram) and theoretical prediction (solid line), compared with that of a Maxwell–Boltzmann distribution with $T = 50$ K (dashed line).

Figure 7 shows the histogram of energies for the sampled King distribution, in good agreement with the theoretical result (solid line) calculated from equation (1) as

$$\rho(E) = f(E)g(E) = f(E) \iint \delta(mv^2/2 - e\Phi(r) - E)\,\mathrm{d}\mathbf{r}\,\mathrm{d}\mathbf{v}.$$

Here $g(E)$ is the classical number of states for the given energy—the phase-space volume occupied by the energy manifold, and f is the distribution function in equation (1).

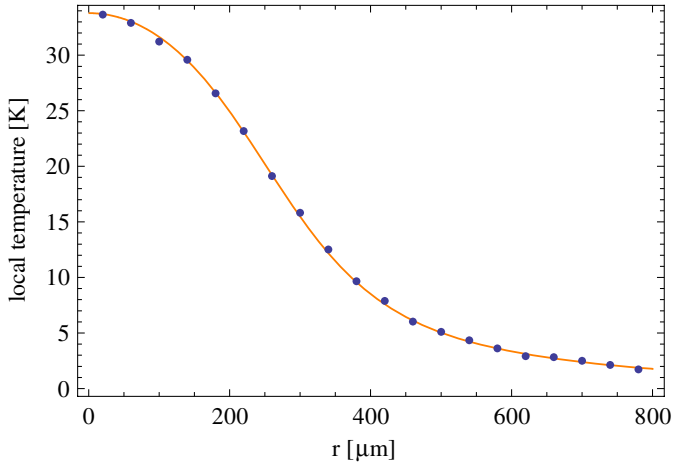

Figure 6. Local temperature variation along the radial direction for the King distribution, for sample (dots) and theoretical prediction (line).

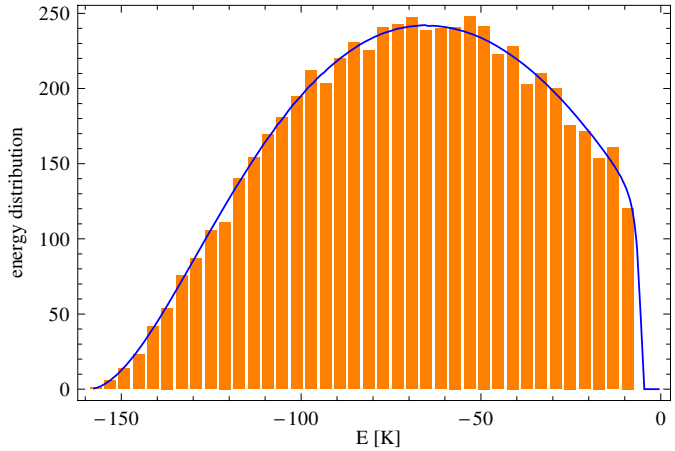

Figure 7. Electron energy distribution for the King distribution: from sampled population (histogram) and theoretical prediction (solid line).

6. Conclusions

A stationary, finite-size distribution is constructed for the electrons in a cloud of fixed ions with a Gaussian density profile. The model is similar to the King model used in astrophysics, but important differences arise from the fact that in a plasma, in contrast to the gravitational case, there are also repulsive forces, apart from the attractive ones.

The distributions can be used as a starting point in molecular dynamics simulations and also in Monte Carlo simulations where working with quasi-equilibrium electron distributions is an essential condition. The King model without space constraints can only exist when the net charge is zero, and for this case the radial density decreases asymptotically as $1/R^{10/3}$.

The electron temperature decreases substantially with increasing distance from the center. One can combine the decrease of density with the one in temperature and evaluate the local

r-dependent rate of TBR using $k_{\mathrm{TBR}} \sim \rho_i \rho_e^2 / T^{9/2}$, as a rough estimate and assuming the validity conditions of the present model.

Acknowledgments

This work has been supported by the US Department of Energy at Los Alamos National Laboratory under contract no. DE-AC52-06NA25396.

References

[1] Killian T C, Pattard T, Pohl T and Rost J M 2007 *Phys. Rep.* **449** 77
[2] Mazevet S, Collins L A and Kress J D 2002 *Phys. Rev. Lett.* **88** 055001
[3] Kuzmin S G and O'Neil T M 2002 *Phys. Plasmas* **9** 3743
[4] Fletcher R S, Zhang X L and Rolston S L 2007 *Phys. Rev. Lett.* **99** 14500
[5] Pohl T, Pattard T and Rost J M 2004 *Phys. Rev.* A **70** 033416
[6] Vanhaecke N, Comparat D, Tate D A and Pillet P 2005 *Phys. Rev.* A **71** 013416
[7] Binney J and Tremaine S 1988 *Galactic Dynamics* (Princeton, NJ: Princeton University Press)
[8] Robicheaux F and Hanson J D 2003 *Phys. Plasmas* **10** 2217
Robicheaux F and Hanson J D 2002 *Phys. Rev. Lett.* **88** 055002
[9] King I R 1966 *Astron. J.* **71** 64
[10] Comparat D, Vogt T, Zahzam N, Mudrich M and Pillet P 2005 *Mon. Not. R. Astron. Soc.* **361** 1227
[11] Pohl T and Pattard T 2006 *J. Phys. A: Math. Gen.* **39** 4571